ACTIVE STICKS - A NEW DIMENSION IN CONTROLLER DESIGN

D. W. Repperger[*], D. McCollor[**]

*   Air Force Aerospace Medical Research Laboratory,
      Wright Patterson Air Force Base, Ohio, 45433

**   Raytheon Service Company

Abstract

In the design of a hand controller, one approach involves a stick with active characteristics. The term active used in this context refers to a control stick which actively exerts a force on the subject's hand so that it may aid in the tracking. Presently, with position type sticks, the human neuromotor bandwidth is limited to 10 radians/second as a consequence of the fact that two sets of muscles (antagonist and agonist) are used to perform neuromotor tracking. When a forearm movement is made in one direction (e.g. laterally) and then reversed, it is necessary to change from one set of active muscles to another set of muscle groups. The additional time to reverse control movements contributes to low levels of neuromotor bandwidth. One method to circumvent this problem and possibly aid in tracking would be to design a stick controller that will perform, partially, the function of some of the muscle groups during the tracking task.

At the Air Force Aerospace Medical Research Laboratory, Wright Patterson Air Force Base, a smart stick controller has been built which actively produces a force to interact with the subject's hand and to aid in tracking. When the human tracks in this situation, the man-machine system can be viewed as the combination of two closed loop feedback paths. The inner loop occurs as a result of a tactile information channel effecting the man-controller interaction through force movements of the stick on the human's hand. The outer feedback loop is a result of the visual display and visual signals. This paper reports the empirical results of tracking with this stick in the active mode (the stick generates a force) and the passive mode (the stick not generating a force). The most noteworthy observation is a significant increase in apparent neuromotor bandwidth and consequently better tracking performance.

Introduction

Much interest has arisen on the comparison of the effects of force versus displacement sticks on pilot tracking ability. Early F-16's were equipped with pure force sticks. Performance improvements occurred when the present limited motion stick replaced the force stick in the F-16. For this stick controller, approximately (1/4") displacement is allowed for a full command input. In an effort to better understand why this occurred and the interaction between force and displacement feedback, a study was conducted a year ago [1] on the performance enhancement of an F-16 style force stick with limited

motion.

In this paper we use a position stick for both the passive (no force applied) and active (force applied to the pilot's hand from the stick) mode of operation. The position information from a stick displacement is sent to a computer. Dynamic restoring forces are sent back from the computer to the operator through the stick via computer control. Our observation that tracking performance improved with a lateral tracking task during lateral acceleration [1] forms the empirical basis to develop a position stick which moves giving force feedback to the operator. We hypothesized that a performance advantage would exist for a position stick which moves with force feedback to the operator in non acceleration environments. To test this hypothesis in a static environment (1Gz), we require (by computer control) the stick to push back on the wrist with a restoring force in a manner similar to the inertial force that would occur in the lateral G environment [1]. From this study it is observed that the unique combination of a visual feedback loop in parallel with a tactile (force feedback) loop figure (7) allows the human to operate the stick controller differently in the active mode as contrasted to the passive mode which only contains visual feedback. This paper reports some performance differences between the active and passive modes of operation. Finally, one additional parameter that was allowed to vary in this study was the electrical gain of the stick (volts output/degree of position of the stick). This variable was allowed to change to see how stick sensitivity effects the usefulness of the device.

The Electro-Mechanical Device

Figure (1) illustrates how the device is constructed. The mass, dashpot, and spring constant were fixed in this study. In general, we consider a device which may have the ability to change K_s, B_s, or M_s in figure (1) but, in addition, adds a biomechanical force directly to the pilot's hand through the control stick. In this sense the controller acts like an active device rather than a passive device. Figure (2) illustrates a system description of the electromechanical device which functions as the smart stick controller. Figure (12) illustrates the actual setup. In figure (2), the output from the computer algorithm drives two current sources I_1 and I_2. These current sources are inputs into two current-pressure transducers to produce pressures p_1 and p_2. The pressure difference $p_1 - p_2$ acting on the area A of the piston produces a force F on the rack and pinion. This force acts through the gear assembly deflecting the stick to the right or the left. The voltage-force characteristics of both of the current pressure transducers are illustrated in figure (3).

To understand the operation of the device, the electrical circuit used to control one current pressure transducer valve is illustrated in figure (4). In figure (4) the winding is inserted in the collector part of the circuit of the transistor using the common emitter configuration. This circuit design protects the windings of the current pressure transducer to a maximum current of (15v-.1)/510 ohms

= 29.2 ma under worst case conditions. The input signal V_{in} enters the base circuit from the computer and on positive swings drives the transistor from the active region into saturation. $V_{in\ max}$ = 10v. from the computer, hence $I_{b\ max}$ = 10v/51K ohms = .2 ma worst case. A clamping diode is inserted to cut off the transistor in the event v_{in} should swing negative and in the cutoff mode of operation I_c = 0. Thus the current-pressure transducer is protected by this current limited circuit arrangement. The common emitter configuration in figure (4) is actually operated in the active mode which is necessary as a result of the non-linear force-voltage input curves illustrated in figure (3). Since the left and right valve both have different characteristics and exhibit hysteresis and dead zone non-linearities, it was decided to bias the transducers about an operating point midway in the linear characteristics curve and to limit the input swings to only linear deviations on the curves in figure (3). To illustrate this point, for the value v_1 (movement right), a bias voltage of 5.3 + (1/2) (swing value) = 5.3 + (1/2)(3.2) = 6.9 volts was chosen as the nominal operating point. The swing voltage about this nominal value was chosen to be $\pm$ 1.6 volts peak to peak (95% of the time), thus ensuring linearity. For valve v_2, the bias value was chosen as 4.3 + (1/2) (1.2) = 4.9 volts with a swing voltage about the nominal of $\pm$ 1.2 volts peak to peak (95% of the time). In this manner both valves produce forces no greater than 3.5 pounds and appear linear within their operating region. Figure (5) illustrates the analog computer diagram relating the computer output of the biomechanical model to the input of the current-pressure transducers. The voltage signal from the computer (output of the biomechanical model) is put into amplifier A_1. The DC bias of 4.9 volts is added as an input to A_1 and goes to the left valve (input to the base circuit in figure (4)).

The Smart Algorithm

In the design of a controller with intelligence, the ability of the controller to perform is a function of the algorithm used in the design of the controller. The smart algorithm could possibly consist of a mathematical representation of an interaction in which improved biomechanical reactions would be obtained in the G acceleration fields. An alternative design would occur if some empirical evidence would support a particular design. In this paper we consider a design which produces inertial forces on the operator similar to those obtained in a previous experiment [1]. Figure (6) illustrates the biomechanical model which represents human response to sidewards accelerations (+Gy direction). The assumption is made that the human arm remains stationary at the elbow. The Gy force acts at the center of mass of the forearm and deflects the arm in the direction of the Gy force which adds a force component at the wrist-stick interface. In static equilibrium the sum of torques about point A in figure (6) is zero. Let F= the force required to compress the spring K_s and dashpot B_s:

Then F = $K_s\ \theta_a\ L_a$ + $B_s\ L_a\ \dot{\theta}_a$ (1)

where the small angle assumption $\theta_a \cong \sin \theta_a$ has been used, θ_a in

figure (6) represents the lateral angular movement of the forearm, and L_a is the length of the forearm. The sum of torques about A = 0 requires:

$$m_a Gy(La) / 2 \quad - \quad F \quad L_a = 0 \tag{2}$$

or combining equations (1) and (2) we have:

$$m_a(1/2) \, G_y = K_s \, \Theta_a + B_s \, \dot{\Theta}_a \tag{3}$$

The transfer function between $\Theta_a(s)$ and $Gy(s)$ is given by:

$$\frac{\Theta_a(s)}{m_a Gy(s)} = \frac{(1/2)}{K_s + B_s \, s} \tag{4}$$

Laplace transforming F from equation (1) yields:

$$F(s) = (K_s + B_s \, s) \, L_a \, \Theta_a(s) \tag{5}$$

$$\text{or:} \quad \frac{F(s)}{m_a \, Gy(s)} = \frac{1}{2} \tag{6}$$

"independent of La,Ks, and Bs". Thus the force necessary at the stick to counteract the G field force is just a constant proportional to the Gy accelerometer measurement. This simplification is derived here as a result of the static equilibrium model considered in this paper.

To complete the design of the smart controller, it is necessary to have some empirical basis by which the man-machine interaction can be improved. From an empirical study run [1] under Gy exposures, two types of biomechanical interaction were defined. Figure (8) illustrates these two types of interaction. Positive Biomechanical Feedthrough is defined such that a stick movement to the right gives rise to a G field in the same direction. This type of interaction accentuates spurious movements and is similar to a closed loop circuit with positive feedback and is undesireable or unstable. The second definition of the biomechanical interaction is what is termed "Negative Biomechanical Feedthrough". In this case the force induced by the G field is in a direction to oppose the original force. This is analogous to negative feedback in an electrical circuit and provides a stablizing influence on the man-machine interaction . Figure (10) illustrates results from [1] in which a comparison was made between static tracking and tracking under the influence of Negative Biomechanical Feedthrough. It was demonstrated that the influence of Negative Biomechanical Feedthrough on tracking performance is significant, especially for fast moving targets. This was the purpose of the design of the smart algorithm considered in this paper.

Implementation of The Device

Figure (7) illustrates the implementation of the device. As the subject makes a stick response (e.g. to the right), this position change is sensed via a circular potentiometer at the base of the stick which generates a voltage signal proportional to the number of degrees of deflection of the stick. This signal is added to a disturbance

722

input forcing function, which is composed of a sum of sine wave signals to simulate wind buffeting or other types of disturbance inputs into the system. The sum of the forcing function disturbance plus stick output becomes the input into an analog computer model of the centrifuge at AFAMRL/ Wright Patterson Air Force Base, Ohio. In this model, the roll dynamics of the cab of the centrifuge (located at the end of a 19 foot radius arm) is given by:

$$\frac{\theta_p(s)}{I(s)} = \frac{1.7}{s + 1.7} \tag{7}$$

where s=1.7 radians/second is the break frequency of the dynamics of this electromechanical system, θ_p is the pointing vector of the cab, and $I(s)$ is the input electrical signal into the cab circuit (output of the amplifier which sums the stick response with the disturbance input forcing function). From this analog model of the centrifuge, $\hat{\theta}_p$ is determined which estimates the postion vector of the cab on the centrifuge. Once $\hat{\theta}_p$ is determined, an estimate of Gy, denoted as $\hat{Gy}$, can be obtained from the equations of motion. Using $\hat{Gy}$, and the static equilibrium model illustrated in figure (6), the force at the center of gravity of the forearm can be determined. Translating this force to the wrist produces the biodynamic interaction on the forearm that would be similar to this G acceleration stress. The purpose of the experiment considered in this paper was to run subjects in the static mode of operation and to try to simulate forces similar to the biodynamic forces that appear on the forearm of the subject for the Negative Biomechanical Feedthrough case illustrated in figure (8b). If the simulation is accurate, then the performance scores when tracking in the static mode of operation with an active stick may improve tracking just as tracking in the dynamic mode (under Gy stress) has demonstrated for the Negative Biomechanical Feedthrough case in figure (10) with a passive stick.

Empirical Validation

A total of 6 subjects were run for the validation of this device. The subjects were all active duty USAF men between the ages of 23 to 35 years. They participated for two days of tracking. On day 1 they tracked for what was considered a training day which consisted of 6 runs with a passive stick (no force on the stick) and 6 runs with the stick active (a simulated Negative Biomechanical Feedthrough force acting on the wrist). Since 4 of the 6 subjects had previous experience with compensatory tracking tasks, the training level was defined as asymptote if we observed less than 5% change in performance scores between similar trials (replications). Three different electrical gain settings of the control stick output were used to assess if stick sensitivity could have had an influence on tracking performance. The choice of the electrical gains was determined [2] from the shape of the spectrum of the forcing function in the frequency domain. Figure (11) illustrates the empirical scores determined across the subjects. For a given controller gain, and for

two out of these three gains, the smart stick improved tracking performance not only significantly, but substantially by a factor of 2 or 3.

Explanation on How The Smart Stick Helps Tracking Performance

To investigate if perhaps some additional information may have been available during the runs of the smart stick and thus provided more information to a subject or perhaps investigate if the smart stick may automatically track the target itself, several tests were made. In Mode 1, the autopilot (an analog simulation) performed the tracking with a passive stick (no stick movement). Its characteristics were specified by:

$$G(s) = (1.7) / (s+1.7) \qquad (8)$$

which replaces the human operator in the loop in figure (7). Mode 2 is the autopilot tracking with the stick active. These results are displayed in Table I. Obviously no difference appears between these two cases. Mode 3 is the open loop mode (no hand on an active stick). Obviously no benefit is derived from lack of human inputs. Mode 4 occurs when the active stick is held at postion zero. Modes 5 and 6, respectively, are the e_{RMS} scores for the passive and active stick when averaged over the 6 subjects. From these runs there appears to be no advantage, information wise, in observing $\hat{\theta}_p$ which is related

Table I Runs To Examine Information in the Loop
(Values of Root Mean Square Error Signal (e_{RMS}))

	Gain 1	Gain 2	Gain 3
Mode 1(Autopilot, Passive Stick)	.019	.019	.019
Mode 2(Autopilot, Active Stick)	.019	.019	.019
Mode 3(Open Loop)	.164	.568	.605
Mode 4(Active Stick Held at Zero)	.034	.115	.318
Mode 5 (mean-Humans, Passive Stick)	.02475	.02463	.0445
(s.d.)	.00132	.00423	.01783
Mode 6 (mean-Humans, Active Stick)	.01725	.01075	.0325
(s.d.)	.00469	.00119	.0139

to the forcing function integrated through two simulations (figure (7)) to appear as the output $\hat{G}y$.
In summary, the subjects had no explicit knowledge of the forcing function disturbance other than implicit information obtained by observing $\hat{\theta}_p$ or $\hat{G}y$.

To better understand why a human tracks better with a smart stick is conjectured in figure (9). Using models akin to optimal control theory [3], typically neuromotor dynamics are modeled via a low pass filter with bandwidth $1/t_N$ and a noise $n(t)$ characterized by $E\{n(t)\} = 0$

and $E\{\eta(t)\ \eta^T(\gamma)\} = Q\ \delta\ (t-\gamma)$ where Q is a covariance matrix representation of human neuromotor noise or tremor. A Weber's law effect is known to occur in which Q scales with tension or force. For example, for twice the force output of the forearm, the noise covariance Q will scale proportionally.

Under the smart stick condition, however, an interesting physiological effect occurs. For normal tracking it is observed that hand movements must be made inward and outward, thus activating both antagonist and agonist muscles. With the smart stick, however, only one type of movement seems to be required. This is because the Negative Biomechanical Feedthrough like effect from our simulation replaces the second group of muscle movements, thus precluding the change in direction and delaying time in switching muscles. Preliminary analysis of these data indicates human operator neuromotor bandwidth increases a factor of 3 using a smart stick and lowers the value of the covariance Q in figure (9) of the noise output. This is the impact on the man-machine system with the use of a smart stick.

Summary and Conclusions

A smart stick has been developed. In tests with a simple lateral tracking task, subject scores were significantly better in the active stick mode than in the passive mode. In both modes, stick position provides the signal to the computer. In the active mode, the stick applies forces at the stick-hand interface that are dynamically similar to the inertial forces that would be generated by the inertia of the forearm if the tracking task were mounted in the AFAMRL human centrifuge. Thus, in the passive mode the subject receives visual target information only. In the active mode there is tactile information providing additional cues about vehicle motion. Serendipitously, the forces generated by the smart stick in the active mode tend to work against major muscle groups, allowing the subject to modulate his muscle force for fine control without the need to reverse direction. This contrasts with the need to continually shift muscle groups and force direction for fine control with a simple position stick in a passive mode of operation.

References

[1] Repperger, D.W., J. W. Frazier, and R. E. Van Patten, "Results From A Biomechanical Stick Study", Proceedings of The 1983 Aerospace Medical Association Meeting, May, 1983, Houston, Texas, pp. 192-193.
[2] Repperger, D.W., D.B. Rogers, J.W. Frazier, and K.E. Hudson, "A Task Difficulty-G Stress Experiment", Vol. 27, No. 2, pp.161-176, Ergonomics, 1984.
[3] Kleinman, D.L., Baron, S., and Levison, W.H., 1971, "A Control Theoretic Approach To Manned-Vehicle System Analysis", IEEE Transactions on Automatic Control, vol. AC-16, pp. 824-832.

List of Variables

I_1, I_2 - Electrical currents into windings (Fig 2)

P_1, P_2-Pressures in gas cylinder (Fig 2)

V_{in}- Voltage into transistor circuit (Fig 4)

I_b - Base Current into transistor (Fig 4)

I_c - Collector Current into transistor (Fig 4)

A_1 - Summing amplifier - (Figure 5)

Gy- Lateral G acceleration force (Fig 6)

F - Force (Fig 6)

K_s - Spring Constant (Fig 6)

θ_a - Angular Deflection of Arm (Fig 6)

L_a - Length of Forearm (Fig 6)

B_s - Dashpot constant (Fig 6)

M_a - Mass of Forearm

s - Laplace Transform Variable

θ_p - Pointing vector of the cab =
      Target position on display

$\wedge$ - estimate of a variable (e.g. $\widehat{Gy}$)

G(s) - Autopilot Transfer function

e_{RMS} - Root Mean Square error

A - Area of piston (Figure 2)

η - human neuromotor tremor

Q - Covariance of η

δ - Dirac delta function

γ - a time $\neq$ t
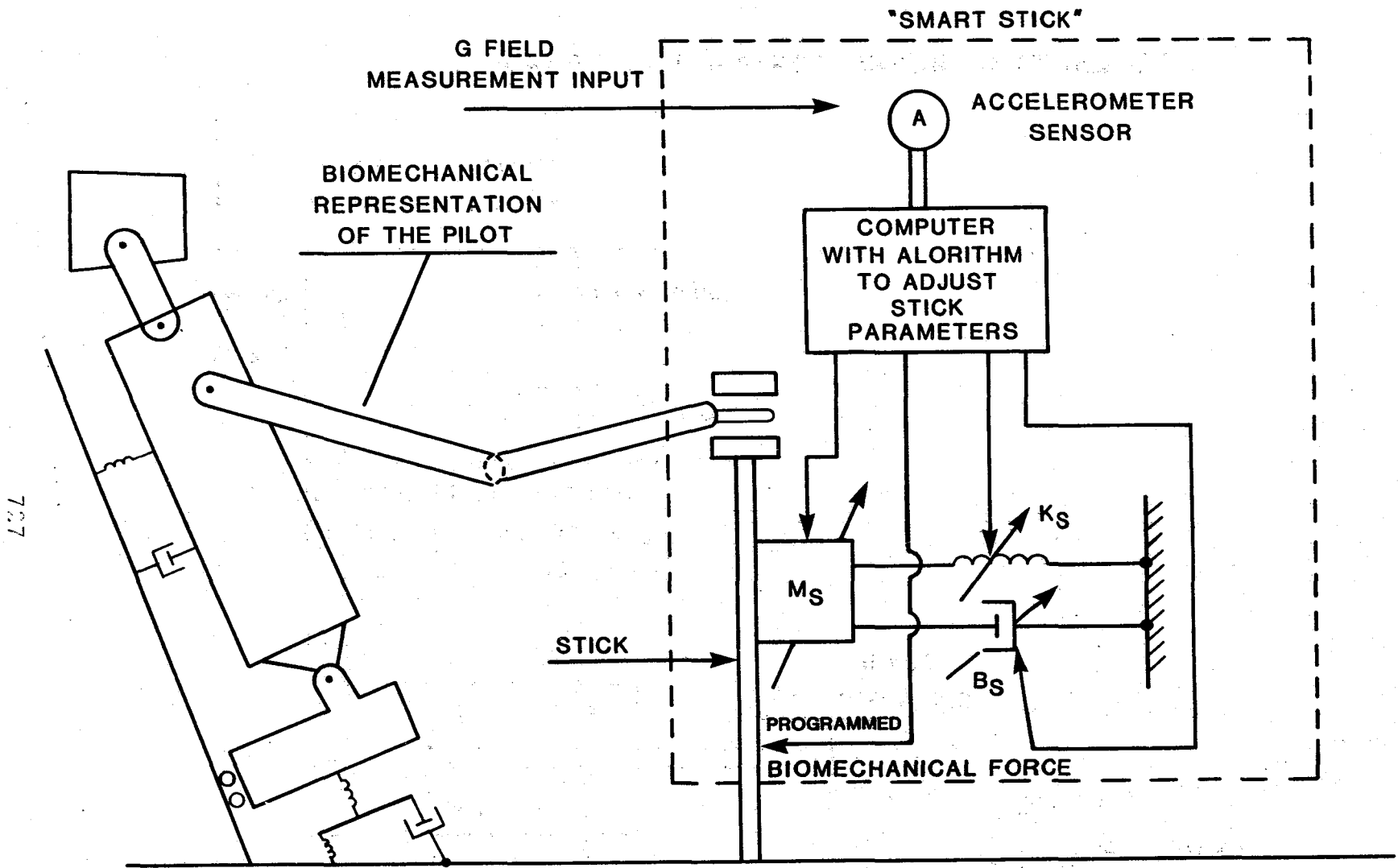
Figure (1) - THE "SMART STICK"
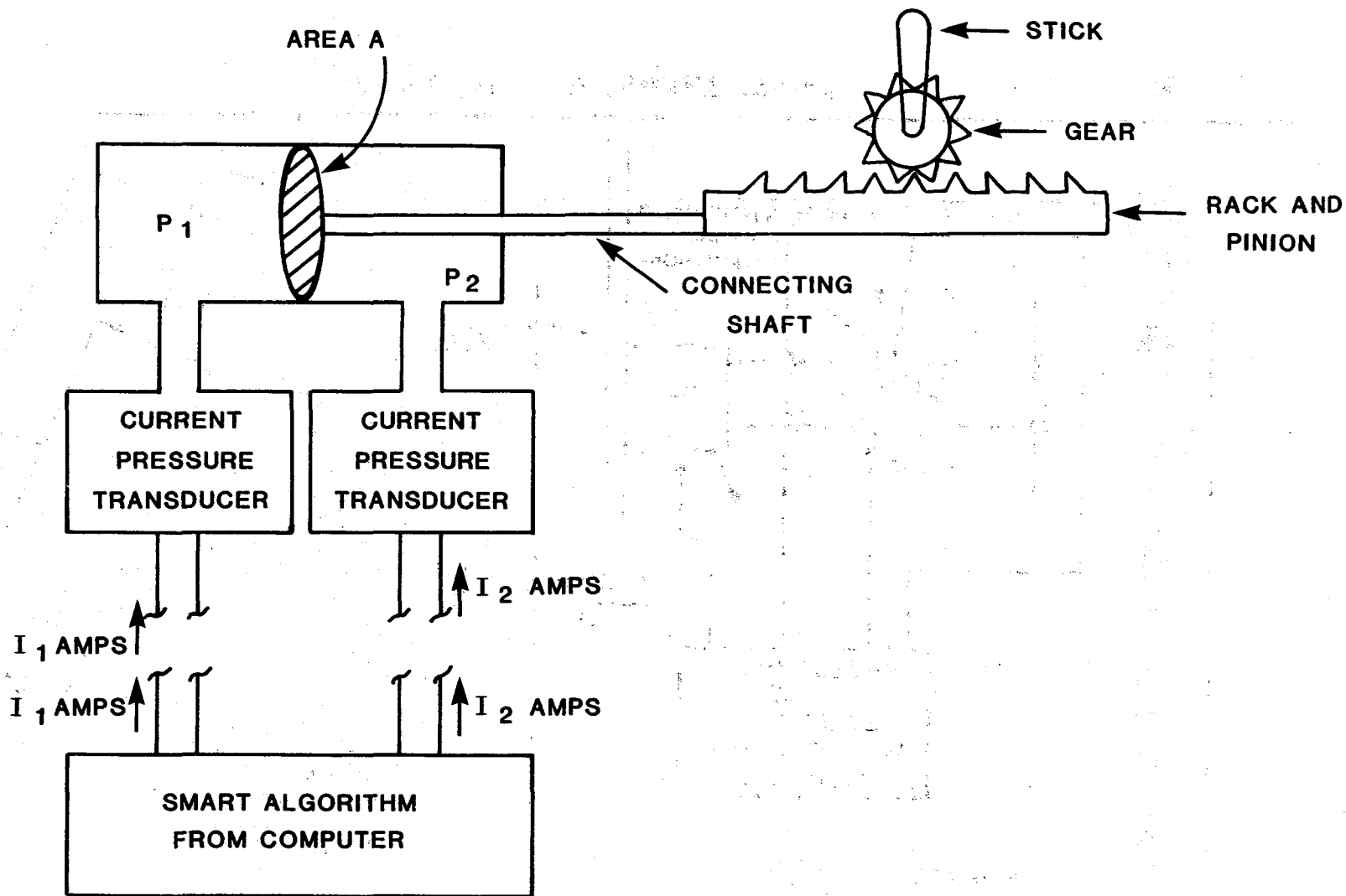
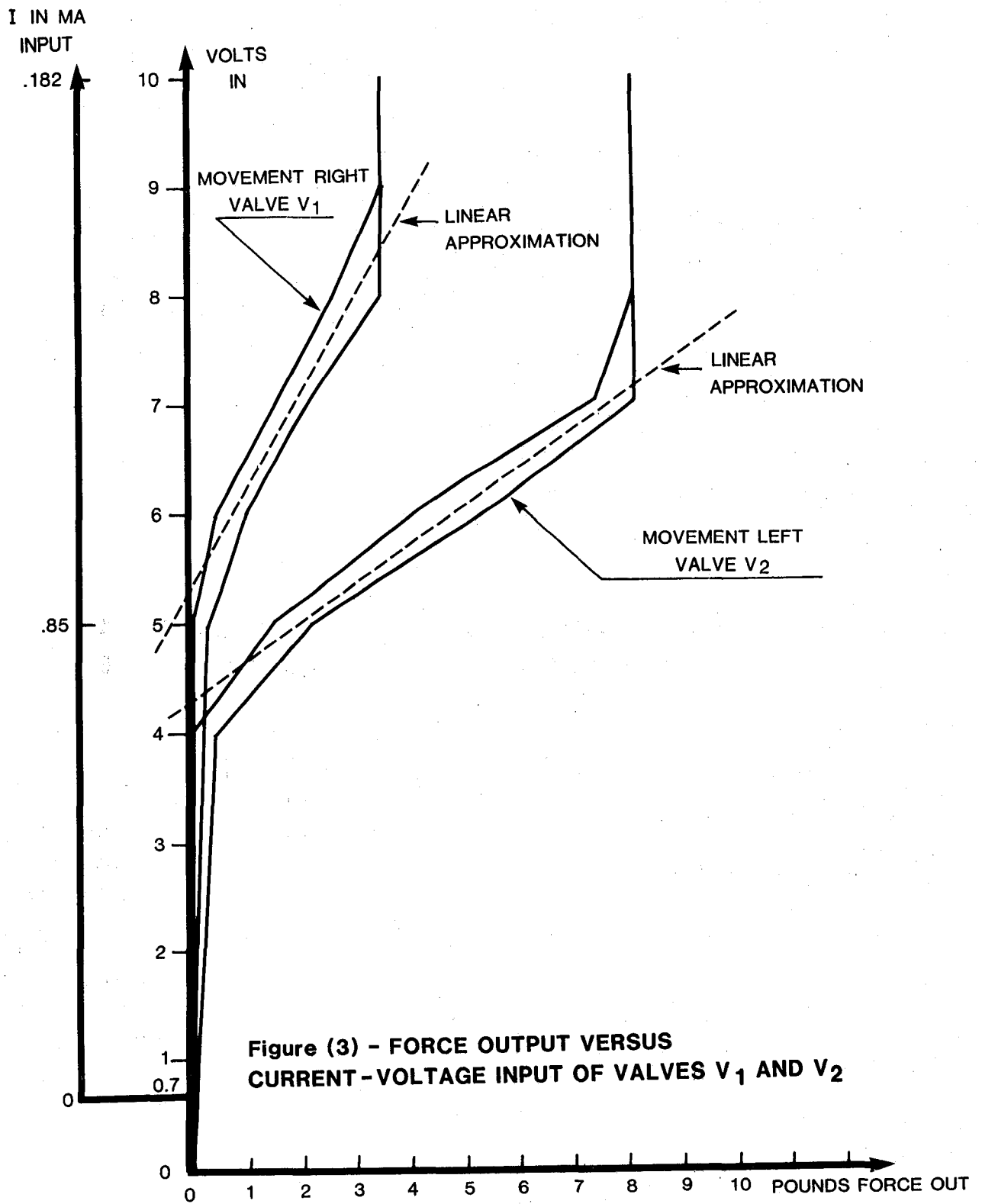Figure (2) – THE ELECTROMECHANICAL DEVICE

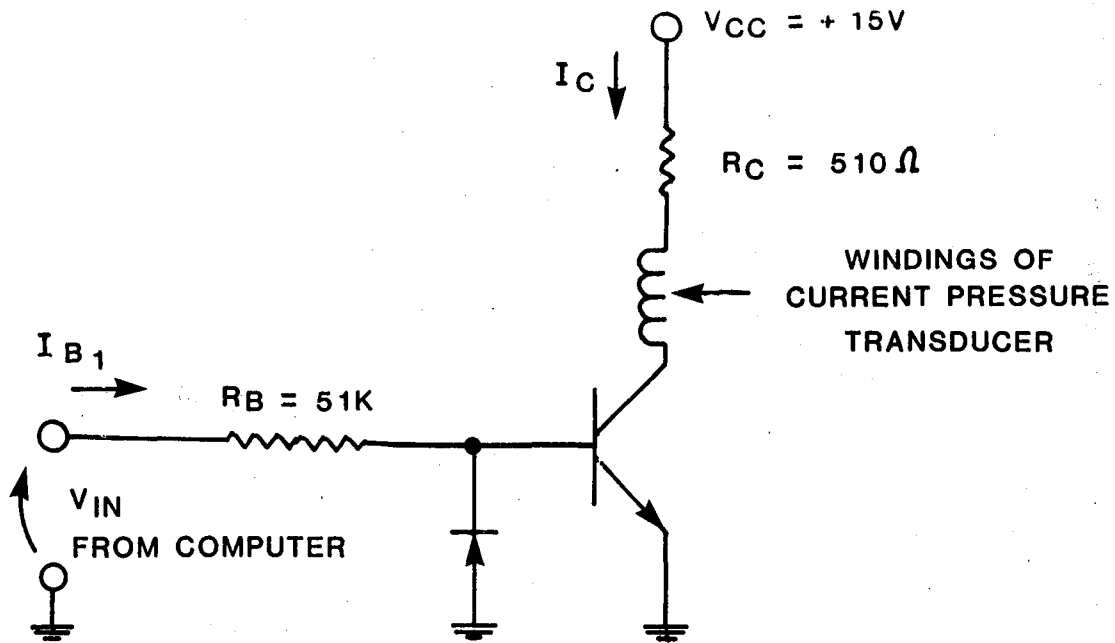Figure (3) – FORCE OUTPUT VERSUS CURRENT-VOLTAGE INPUT OF VALVES V_1 AND V_2

Figure (4) - THE CURRENT LIMITED ELECTRICAL CIRCUIT TO DRIVE THE CURRENT-FORCE TRANSDUCER
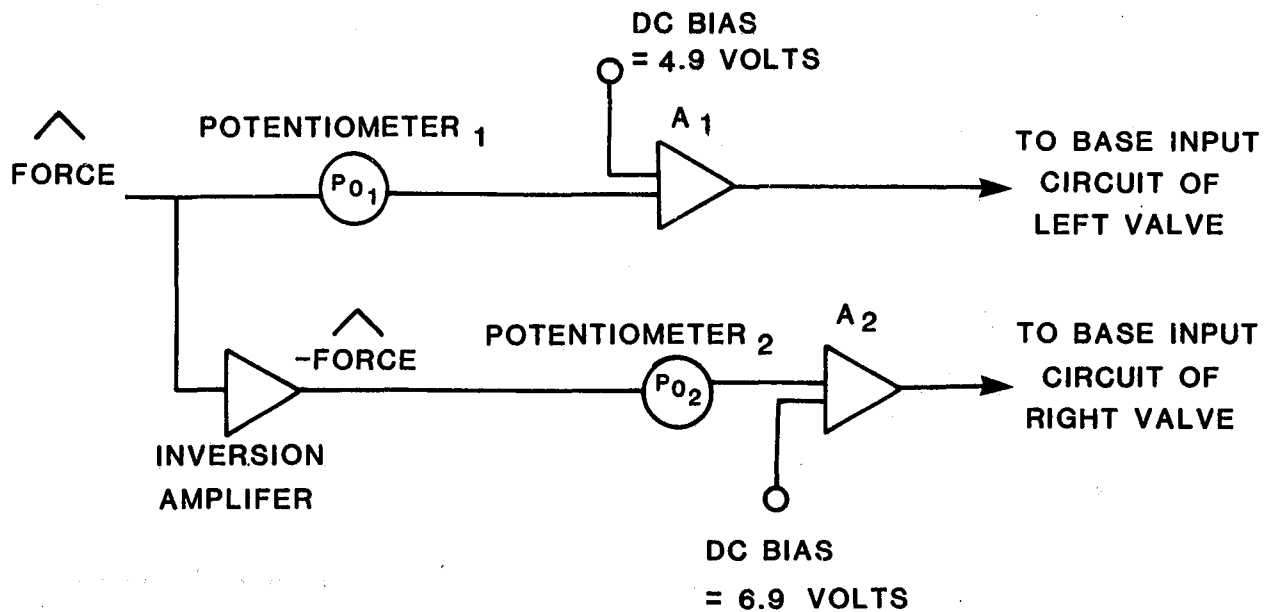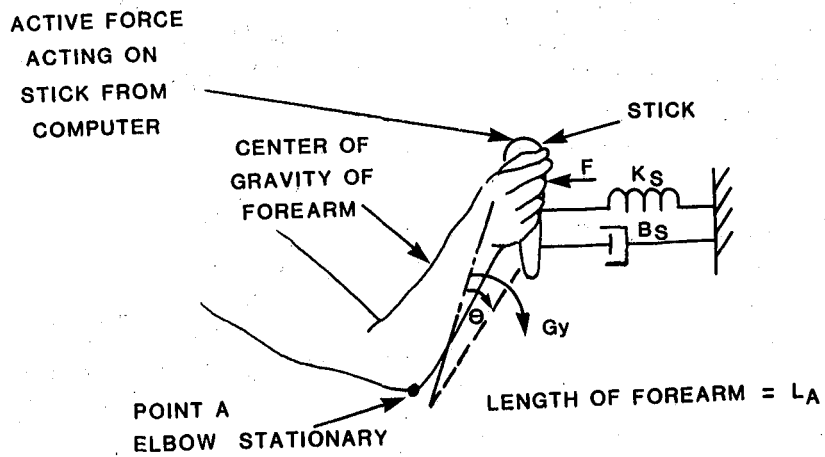

Figure (5) - THE ANALOG COMPUTER DIAGRAM
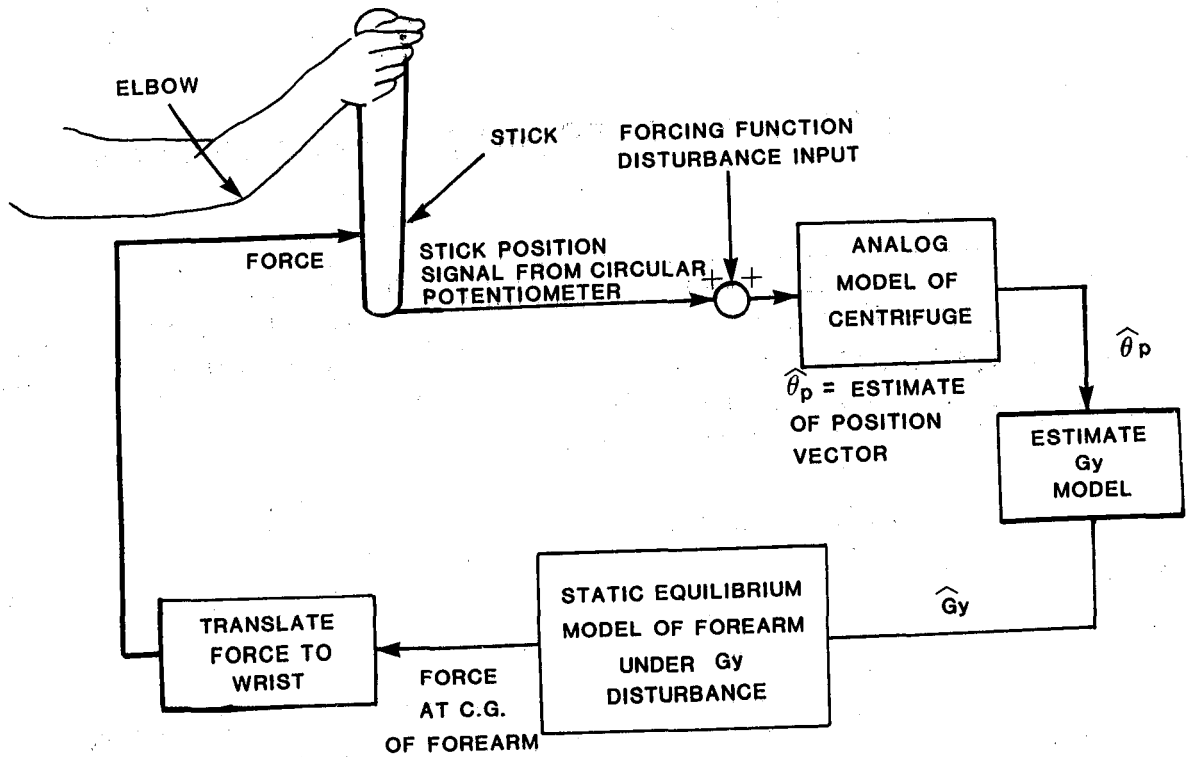
Figure (6) - THE BIOMECHANICAL MODEL

Figure (7) - IMPLEMENTATION OF SMART STICK

INDUCED G FIELD
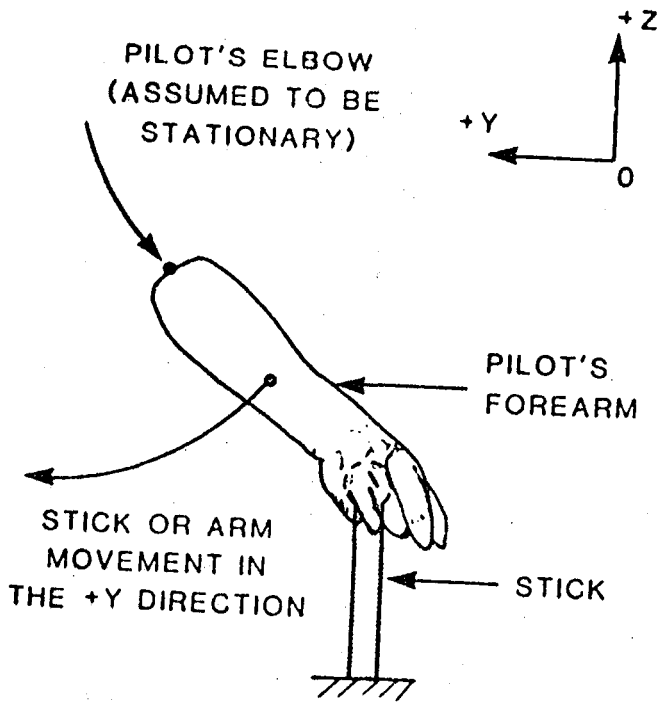IN THE +Y DIRECTION
AS A RESULT OF THE
ARM MOVEMENT

G FIELD INDUCED

PILOT'S ELBOW
(ASSUMED TO BE
STATIONARY)

+Z

+Y

0

PILOT'S
FOREARM

STICK OR ARM
MOVEMENT IN
THE +Y DIRECTION

STICK

Figure {8a}

POSITIVE BIOMECHANICAL FEEDTHROUGH

INDUCED G FIELD
IN THE -Y DIRECTION
AS A RESULT OF THE
ARM MOVEMENT

G FIELD INDUCED

PILOT'S ELBOW
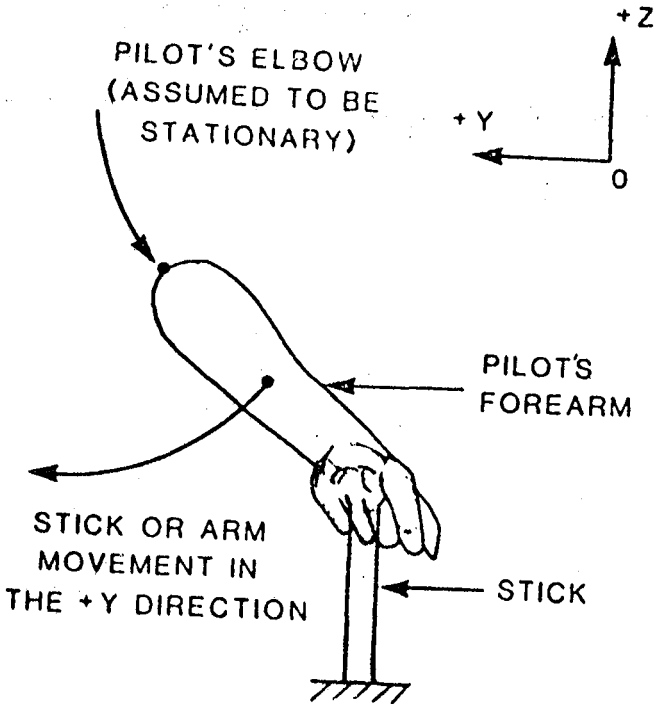(ASSUMED TO BE
STATIONARY)

+Z

+Y

0

PILOT'S
FOREARM

STICK OR ARM
MOVEMENT IN
THE +Y DIRECTION

STICK

Figure {8b}

NEGATIVE BIOMECHANICAL FEEDTHROUGH

H(s)

TRANSFER FUNCTION

$$\frac{1}{1+S\tau_N}$$

$1/\tau_N$

NOISE
$\eta\,(t)$

INPUT
SIGNAL

H(s)

$+$

$+$

OUTPUT
VARIABLE

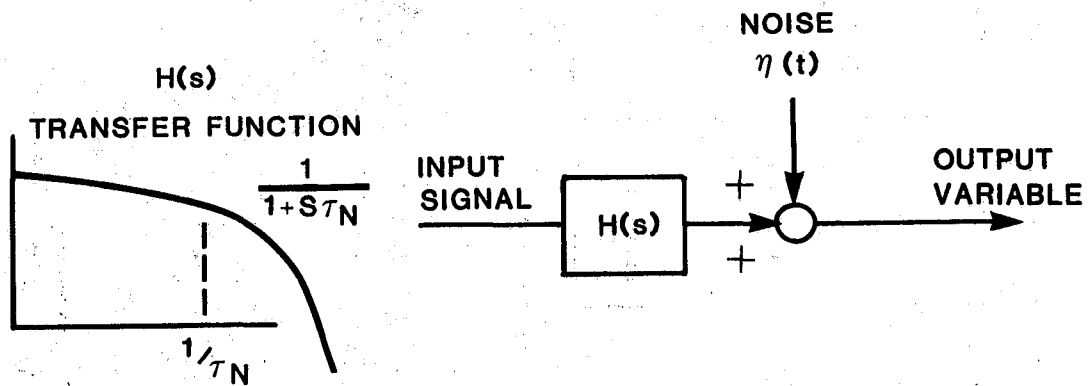**Figure (9) – AN INFORMATION CHANNEL REPRESENTATION OF NEUROMOTOR DYNAMICS**

E Root Mean Square
Averaged across 6 subjects

.048
.044
.040
.036
.032
.028
.024
.020
.016
.012
.008
.004
0

Passive Stick

Smart Stick

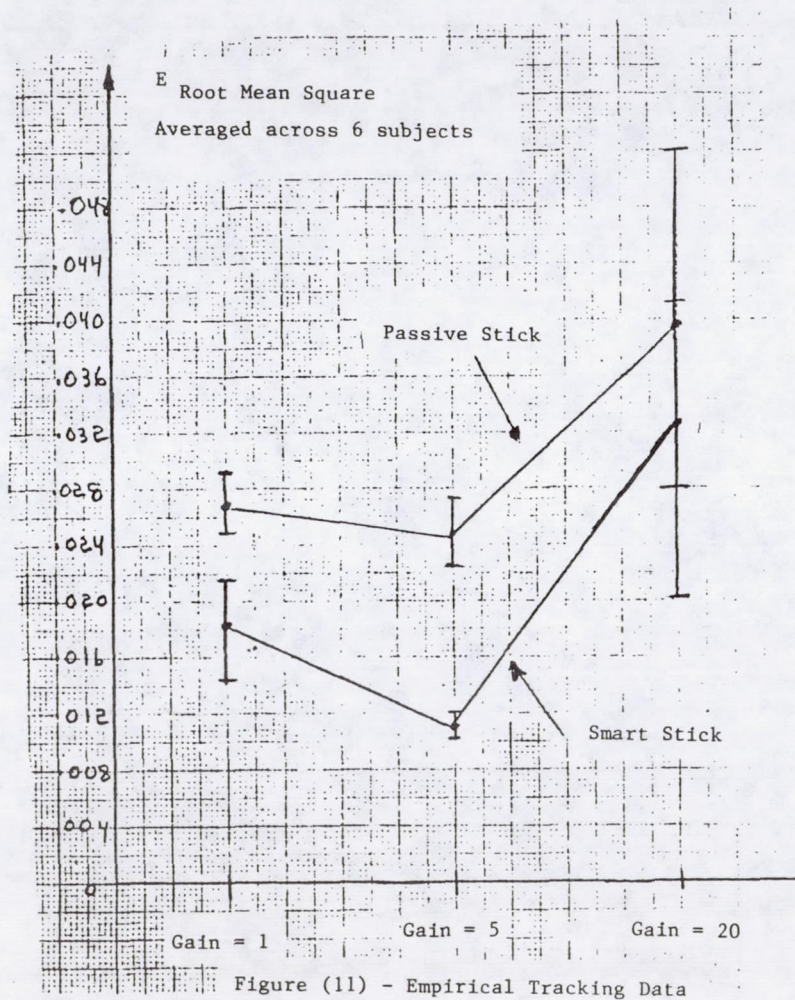Gain = 1   Gain = 5   Gain = 20

Figure (11) - Empirical Tracking Data

—— STATIC
---- NEGATIVE BIOMECHANICAL FEEDTHROUGH

e_{RMS}

Ke=1   Ke=5   Ke=20

0.5
0.4
0.3
0.2
0.1
0.0

STICK
NUMBER

1   2   3   1   2   3   1   2   3
Ks_1 Ks_2 Ks_3 Ks_1 Ks_2 Ks_3 Ks_1 Ks_2 Ks_3

Figure (10)

Figure (12) - The Device